DOI: 10.1002/chem.201000526

Tuning the Spin States of Two Apical Iron(II) Ions in the Trigonal-Bipyramidal $[\{Fe^{II}(\mu\text{-bpt})_3\}_2Fe^{II}{}_3(\mu_3\text{-O})]^{2+}$ Cations Through the Choice of Anions

Xin Bao,[a] Ji-Dong Leng,[a] Zhao-Sha Meng,[a] Zhuojia Lin,[a] Ming-Liang Tong,*[a] Masayuki Nihei,[b] and Hiroki Oshio*[b]

When located in octahedral environment, the iron(II) ion with a d^6 electronic configuration may adopt two different stable electronic states, namely, a diamagnetic low-spin (LS) state and a paramagnetic high-spin (HS) state, which both give rise to different magnetic, optical and electronic properties. So tuning the spin state of the iron(II) ion is significant and contributes to the development of amazing materials that can be used as molecular switches, sensors and display devices.[1] As is well established, the spin state depends on relative strength of spin paring energy (P) and splitting energy (Δ_0). If the former is much stronger than the latter, the HS state will be stabilised, and if Δ_0 is stronger then the LS state will be the ground state. If P and Δ_0 are comparable a spin crossover (SCO) may occur between the HS and LS state by external perturbations such as temperature, pressure or light irradiation. So the main task is to make a judicious choice of ligand, which can impose a proper ligand-field strength.[2] However, in reality, the spin state of the iron(II) ion is quite sensitive to even more subtle changes such as solvent molecules,[3] polymorphism[4] and counterions.[5]

As one of the best representatives of switchable molecules, SCO materials have attracted considerable interest in the chemistry and materials fields. Current work mainly focuses on the enhancement of cooperativity, which results in an abrupt transition and a wider thermal hysteresis.[6] Another promising research area, but with few examples,[7] is the combination of magnetic-exchange and spin-transition (ST) phenomena in the same molecule or polymeric network, which could eventually afford new switching materials with considerable amplification of the response signal.[1d] Much more work should be done to expand our knowledge of spin electronics.

To induce a ST, the most common method is by varying the temperature. However, light-and pressure-induced SCOs play an increasingly important role owing to their potential applications as optical and pressure switches, for example. Moreover, the latter two methods are not restricted to thermal SCO compounds: LIESST (light-induced excited spin-state trapping) may also be observed in LS compounds, whereas HS compounds may experience STs with the application of external hydrostatic pressure.

Although there are many examples that exhibit thermal STs, rare spin-crossover clusters of iron(II) have been found to exhibit a mixed-spin structure and synergy between ST and magnetic interaction. Fortunately, by introducing counterions, we have successfully tuned the spin states of two apical iron(II) ions in the pentanuclear $[\{Fe^{II}(\mu\text{-bpt})_3\}_2Fe^{II}{}_3(\mu_3\text{-O})]^{2+}$ (Hbpt = 3,5-bis(pyridin-2-yl)-1,2,4-triazole) cations through anions. Both apical ions are of LS states in $[\{Fe^{II}(\mu\text{-bpt})_3\}_2Fe^{II}{}_3(\mu_3\text{-O})](NCS)_2{\cdot}10H_2O$ (**1**), $[\{Fe^{II}(\mu\text{-bpt})_3\}_2Fe^{II}{}_3(\mu_3\text{-O})](ClO_4)_2{\cdot}3H_2O$ (**2**) and $[\{Fe^{II}(\mu\text{-bpt})_3\}_2Fe^{II}{}_3(\mu_3\text{-O})]I_2{\cdot}4MeCN$ (**3**), and are of HS states in $[\{Fe^{II}(\mu\text{-bpt})_3\}_2Fe^{II}{}_3(\mu_3\text{-O})][Fe^{III}{}_2(\mu\text{-O})Cl_6]{\cdot}{}^1/_2H_2O$ (**4**). In this new $\{Fe_5\}$ family, two new developments have been achieved: 1) The ligand 4-amino-3,5-bis(pyridine-2-yl)-1,2,4-triazole (abpt) has been, for the first time, used to produce the oxo-centred polynuclear iron(II) complexes;[8a–d] 2) Two types of spin topology have been trapped in the $[\{Fe^{II}(\mu\text{-bpt})_3\}_2Fe^{II}{}_3(\mu_3\text{-O})]^{2+}$ cluster that are controlled by counterions. Note that only one

[a] X. Bao, J.-D. Leng, Z.-S. Meng, Dr. Z.-J. Lin, Prof. Dr. M.-L. Tong
Key Laboratory of Bioinorganic and
Synthetic Chemistry of Ministry of Education
State Key Laboratory of Optoelectronic Materials and Technologies
School of Chemistry & Chemical Engineering
Sun Yat-Sen University, Guangzhou 510275 (P.R. China)
Fax: (+86) 20-8411-2245
E-mail: tongml@mail.sysu.edu.cn

[b] Dr. M. Nihei, Prof. Dr. H. Oshio
Graduate School of Pure and Applied Sciences
University of Tsukuba, Tennodai 1-1-1, Tsukuba 305-8571 (Japan)
Fax: (+81) 29-853-4238
E-mail: oshio@chem.tsukuba.ac.jp

Supporting information for this article is available on the WWW under http://dx.doi.org/10.1002/chem.201000526.

pentanuclear Fe^{II} complex containing a $[\{Fe^{II}(\mu\text{-}L)_3\}_2Fe^{II}{}_3(\mu_3\text{-}O)]^{2+}$ core similar to those of **1** to **4** has been reported by Kawata et al. from the reaction of $FeCl_2{\cdot}4H_2O$ with 3,5-bis-(pyridin-2-yl)pyrazole (HL) in the presence of NaNCS under an N_2 atmosphere.[8e]

Single-crystal X-ray diffraction measurements were carried out at 293 and 100 K for **1**, at 308 and 150 K for **2**, and at 293 and 150 K for **3**. No significant change in their respective cell dimensions was noticed at the two temperatures. Neither phase transition nor change in the iron spin states was observed. Therefore, only the structures at low temperature will be discussed in detail. Relevant crystallographic data are collected in Table 1. Although **1**, **2** and **3** were crystallised with different counterions and solvent molecules, the pentanuclear cations $[\{Fe^{II}(\mu\text{-bpt})_3\}_2Fe^{II}{}_3(\mu_3\text{-}O)]^{2+}$ are essentially the same. As shown in Figure 1, the cation geometry is that of a trigonal bipyramid in which two LS Fe^{II} ions ($S=0$) occupy the apical positions and three HS Fe^{II} ions ($S=2$) are connected by a μ_3-O atom reside in the equatorial plane. Three pairs of bis-bidentate bpt^- ligands with offset face-to-face π–π stacking are arranged around the pentanuclear core. Each pair of apical and equatorial ions is bridged by two N atoms from the bpt^- ligands and thus form a triple-stranded helical configuration, but the complex is racemic owing to pairs of enantiomers present in the crystal. Both of the apical ions assume an octahedral coordination environment with six N-donor atoms from three chelating ligands. Each iron centre at the equatorial position is in an N_4O trigonal pyramidal environment that is trigonally distorted ($\tau=0.68$–0.80 for **1**–**3**, Table 1) and is surrounded by one O^{2-} ion and four N atoms from two chelating bpt^- ligands.

Table 1. Average Fe–N and Fe–O bond lengths [Å], parameter Σ [°] and parameter τ [°] at different temperatures.

	1 (100 K)	2 (150 K)	3 (150 K)	4 (100 K)
$Fe-N_{apical}$	1.98	1.99	1.97	2.20
$Fe-N_{equatorial}$	2.18	2.16	2.17	2.15
$Fe-O_{equatorial}$	1.89	1.88	1.89	1.85
Σ_{apical}	Fe(3), 64.07	Fe(4), 60.2 Fe(5), 60.2	Fe(3), 58.40	Fe(4), 108.22 Fe(5), 103.82
$\tau_{equatorial}$	Fe(1), 0.80 Fe(2), 0.76	Fe(1), 0.74 Fe(2), 0.68 Fe(3), 0.72	Fe(1), 0.76 Fe(2), 0.75	Fe(1), 0.60 Fe(2), 0.70 Fe(3), 0.64

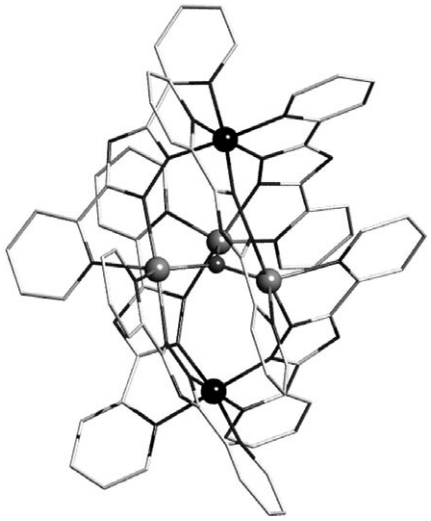

Figure 1. Ball-and-stick representation of the $[\{Fe^{II}(\mu\text{-bpt})_3\}_2Fe^{II}{}_3(\mu_3\text{-}O)]^{2+}$ cation (H atoms are omitted for clarity) in **1**, **2** and **3**. LS Fe^{II} and HS Fe^{II} ions are in black and grey, respectively.

Single-crystal X-ray structural analysis at 293 and 100 K reveals that **4** crystallises in the $P2_1/c$ space group. As for **1**–**3**, no phase transition was observed in **4**. Therefore, only the low-temperature structure will be discussed in detail. Complex **4** contains $[\{Fe^{II}(\mu\text{-bpt})_3\}_2Fe^{II}{}_3(\mu_3\text{-}O)]^{2+}$ cations that are quite similar to those of **1**–**3**, $[Fe^{III}{}_2(\mu\text{-}O)Cl_6]^{2-}$ anions and disordered solvated water molecules (Figure 2). To our great surprise, compared with those of **1**–**3**, the two apical Fe^{II} ions in **4** experienced spin transitions to HS states ($S=2$) with an average Fe_{apical}–N bond length of 2.20 Å, although the essential structure of the pentanuclear cation in **4** is, at first view, almost same as those in **1**–**3**. A decrease of the ligand-field strength in **4** probably originates from the change of counterions, which leads to three significant changes: 1) Weaker hydrogen bonds in the form of C–H···Cl instead of C–H···O/N/S in **1**–**3** are found (see Tables S1–4 in the Supporting Information). Hydrogen bonds can directly influence the electronic configuration of metal ions[9] and will generally stabilise the LS state.[10,3f,5b] Because Cl atoms are worse hydrogen-bond acceptors than O/N atoms, the electron densities of bpt^- ligands in **4** are lower compared with the previous three, leading to weakening of the N–Fe σ bonds; 2) The π–π stacking interactions between adjacent clusters were only observed in **4**, which may play a subtle role in tuning the spin states of Fe^{II} ions; 3) Compared with **1**–**3**, apical iron ions in **4** show more distorted octahedral geometries (the octahedron distortion parameter $\Sigma=|90-\theta|$ (°), in which the θ value is the bite angle of the two coordinated ligands).[11] A larger Σ value, which signifies larger distortion from the ideal octahedral coordination sphere, corresponds to a weaker ligand-field strength on an iron(II) ion. The relatively large Σ values of 108.22 and 103.82° for the two apical iron(II) ions in **4** suggest that the iron(II) ions are in the HS state at 100 K (Table 1). Similar observations have been previously reported.[12,3c,g]

Variable-temperature (2–300 K) magnetic susceptibility measurements in a 500 Oe field were obtained for **1** and **4**. As shown in Figure 3a, the $\chi_M T$ value of **1** is 3.74 $cm^3 K mol^{-1}$ at 300 K, which is much smaller than the spin-only value (9.0 $cm^3 K mol^{-1}$) for three noninteracting HS iron(II) ions, by assuming an isotropic g value of 2.00.[13] When lowering the temperature, the $\chi_M T$ product decreases monotonically to 0.065 $cm^3 K mol^{-1}$ at 2 K. This behaviour confirms the presence of strong antiferromagnetic coupling in the trianglular $[(Fe_{HS})^{II}{}_3(\mu\text{-}O)]^{4+}$ core. Fitting the experimental curve by using the isosceles triangle Hamiltonian

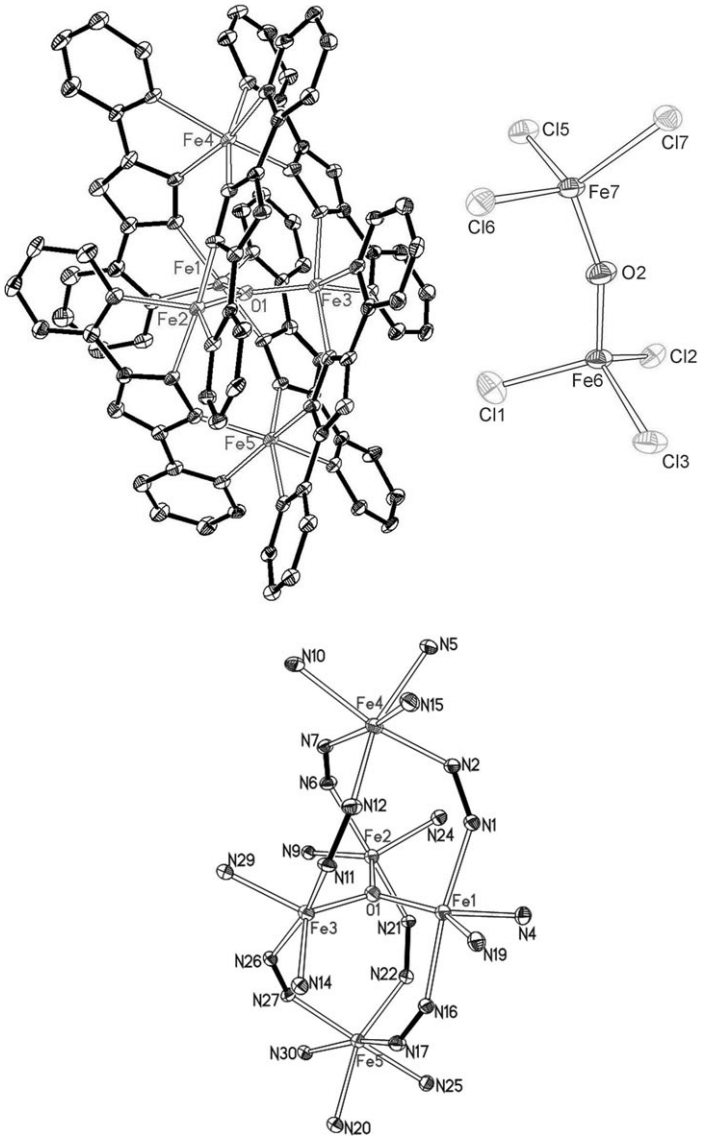

Figure 2. ORTEP drawings of the structure (top) and the coordination environment of the metal ions (bottom) in **4** displaying 30% thermal ellipsoids.

$\mathscr{H} = -2[J_1(S_{Fe1}S_{Fe2}) + J_1(S_{Fe1}S_{Fe2a}) + J_2(S_{Fe2}S_{Fe2a})]$ gives $J_1 = -40.3\ cm^{-1}$, $J_2 = -52.7\ cm^{-1}$ and $g = 2.28$ (Figure 3a). The larger J values indicate stronger interactions than those ($J = -29.0\ cm^{-1}$, $g = 2.29$) reported by Kawata et al.,[8e] which has a similar $[(Fe_{HS})^{II}{}_3(\mu\text{-}O)]^{4+}$ core.[8e] Two examples with Fe^{II}–O–Fe^{II} antiferromagnetic interactions show that the antiferromagnetic exchange in this path is usually stronger than those found in the Mn^{III}–O–Mn^{III} series,[14] probably due to an extra unpaired electron contributing to the antiferromagnetic exchange pathways.[8e]

The $\chi_M T$ value for **4** drops from $12.48\ cm^3\,K\,mol^{-1}$ at 300 K to $4.43\ cm^3\,K\,mol^{-1}$ at 2 K, indicating significant antiferromagnetic coupling. The room-temperature value is much lower than expected ($23.75\ cm^3\,K\,mol^{-1}$) for seven isolated metal ions ($5Fe_{HS}^{II} + 2Fe_{HS}^{III}$). Compared with **1**, the

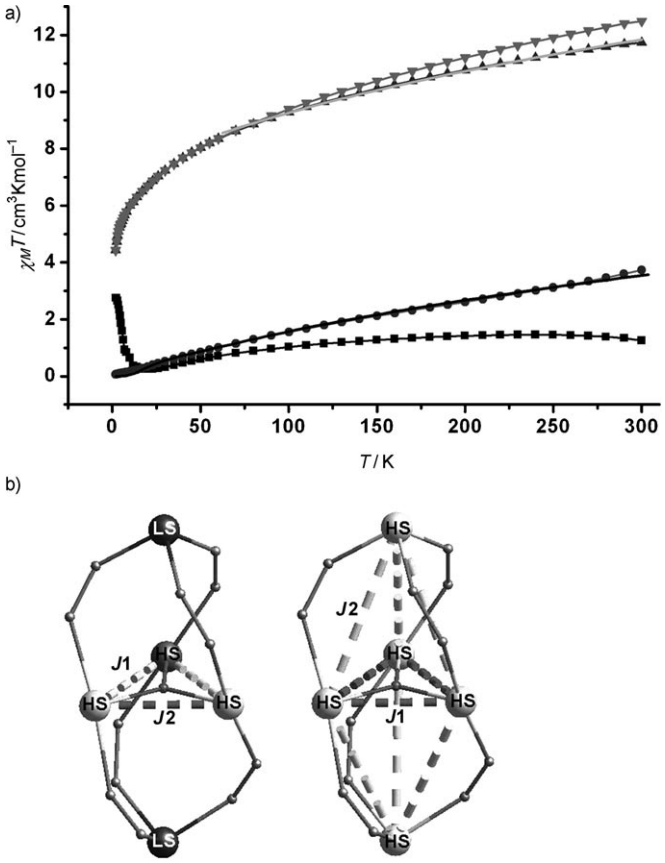

Figure 3. a) Plots of $\chi_M T$ vs. T for **1** (●), **4** (▼), the $[\{Fe_{HS}^{II}(\mu\text{-bpt})_3\}_2(Fe_{HS})^{II}{}_3(\mu\text{-O})]^{2+}$ cation (▲), the interaction plot between the $[(Fe_{HS})^{II}{}_3(\mu\text{-O})]^{4+}$ core and two apical Fe_{HS}^{II} ions (■) in **4** and experimental fittings for **1** (black solid line) and **4** (light grey solid line). b) Magnetic exchange coupling pathways in the pentanuclear cation of **1** (left) and **4** (right).

magnetic interactions are much more complicated in **4** owing to the contribution of $[(Fe_{HS})^{III}{}_2OCl_6]^{2-}$ anion as well as two apical Fe_{HS}^{II} ions. What interested us most was to clarify the type of interaction in the trigonal-bipyramidal cluster, so in a first step, the contribution of $[(Fe_{HS})^{III}{}_2OCl_6]^{2-}$ anion must be excluded. Fortunately, the magnetic properties of the anion have been well studied.[15] Regardless of the weak interactions between the anion and the pentanuclear cation, we get the magnetic susceptibility plot of the $[\{Fe_{HS}^{II}(\mu\text{-bpt})_3\}_2(Fe_{HS})^{II}{}_3(\mu_3\text{-O})]^{2+}$ core by subtracting the plot of the anion (neglecting the drop at low temperatures). It has a similar profile to **4** with a room-temperature value of $11.73\ cm^3\,K\,mol^{-1}$, which is smaller than the spin-only value ($15.0\ cm^3\,K\,mol^{-1}$) of five high-spin iron(II) ions, also indicating an overall antiferromagnetic coupling within the trigonal bipyramidal cluster.

But it is still difficult to conclude the nature of the magnetic interaction exhibited between the $[(Fe_{HS})^{II}{}_3(\mu_3\text{-O})]^{4+}$ core and the apical ions only from the shape of the $\chi_M T$ versus T curve owing to the strong antiferromagnetic interaction in the trianglular core. One method to solve the problem is to obtain the pure interaction ($\Delta\chi_M T$ vs. T) plot.[16] Therefore, in a second step, we subtracted the contribution

of the $[(Fe_{HS})^{II}_3(\mu_3\text{-}O)]^{4+}$ core and the paramagnetic contribution from two apical Fe_{HS}^{II} ions[17] ($\Delta\chi_M T = \chi_M T([\{(Fe_{HS})^{II}_3(\mu\text{-bpt})_3\}_2(Fe_{HS})^{II}_3(\mu_3\text{-}O)]^{2+}) - 2\chi_M T(Fe_{HS}^{II}) - \chi_M T([(Fe_{HS})^{II}_3(\mu_3\text{-}O)]^{4+})$). The pure interaction plot is shown in Figure 3a, which shows an overall ferrimagnetic coupling. For now we conclude that the interaction between the apical Fe_{HS}^{II} ions and the equatorial $[(Fe_{HS})^{II}_3(\mu_3\text{-}O)]^{4+}$ core is antiferromagnetic.

To obtain quantitative estimates of the intracluster exchange interactions, we restricted our fits of the data to theoretical trigonal-bipyramidal models. Considering the two kinds of bridging group and the similar Fe–Fe distances in each group, two exchange interaction parameters (J_1, J_2) were proposed, in which J_1 defines the exchange interaction between the equatorial ions bridged by an O^{2-} anion, and J_2 represents the interaction between the apical and equatorial ions bridged by triazole (Figure 3b). This exchange coupling scheme results in the spin-only isotropic Heisenberg Hamiltonian given in [Eq (1)].

$$\mathscr{H} = -2J_1(S_{Fe1}S_{Fe2} + S_{Fe1}S_{Fe3} + S_{Fe2}S_{Fe3}) - 2J_2S_{Fe4}(S_{Fe1} + S_{Fe2} + S_{Fe3}) - 2J_2S_{Fe5}(S_{Fe1} + S_{Fe2} + S_{Fe3}) \quad (1)$$

Thus we plotted the $\chi_M T$ versus T plot above 60 K by using the above model resulting in $J_1 = -31.07\ cm^{-1}$, $J_2 = -0.68\ cm^{-1}$ and $g = 2.26$, in which J_1 and g are comparable with those reported in reference [8e], and J_2 is in agreement with the antiferromagnetic interaction between the apical ions and the equatorial $[(Fe_{HS})^{II}_3(\mu_3\text{-}O)]^{4+}$ core.

To characterise the low-temperature magnetic properties of **1** and **4** further, magnetisation measurements were carried out at 2 K in fields up to 70 kOe (see Figure S6 in the Supporting Information). At our lowest temperature of 2 K the molar magnetisation (M) of complexes **1** and **4** reached values of only 0.17, 5.52 Nβ, respectively, even in 70 kOe. For non-interacting metal ion spins such a field/temperature combination would be sufficient to approach the saturation value of 12 and 30 Nβ ($M = gS_T N\beta$). This is strong evidence for the presence of antiferromagnetic interactions.

The ^{57}Fe Mössbauer spectra of **1** and **4** were measured at 20 K to characterise the spin state of the iron centre. The Mössbauer parameters were calculated relative to metal iron and were summarised in Tables S5 and S6. The Mössbauer spectrum of **1** is composed of three quadrupole doublets (HS1 and HS2 in red, and LS1 in blue; Figure 4a and Table S5 in the Supporting Information). The peak-area ratio of HS1, HS2 and LS1 was estimated to be 0.21:0.38:0.41. The Mössbauer parameters of two doublets (HS1 and HS2) are $\delta = 0.99$ and $\Delta E_Q = 2.80\ mm\,s^{-1}$ and $\delta = 0.97$ and $\Delta E_Q = 2.28\ mms^{-1}$, respectively, which are characteristic of HS Fe^{II} ions. The doublet LS1 has Mössbauer parameters of $\delta = 0.44$ and $\Delta E_Q = 0.28\ mms^{-1}$, which are typical values for LS Fe^{II} ions. Consequently, HS1 and HS2 are assigned to Fe^{II} ions in the $[Fe_3(\mu_3\text{-}O)]$ core, and LS1 corresponds to two apical Fe^{II} ions. In the Mössbauer spectrum of

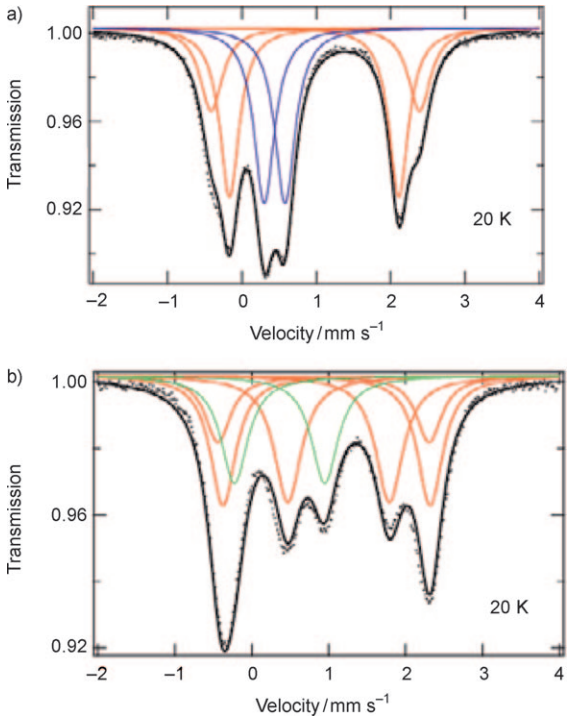

Figure 4. Mössbauer spectra of a) **1** and b) **4** at 20 K.

4 at 20 K (Figure 4b and Table S6 in the Supporting Information), four quadrupole doublets (HS1, HS2 and HS3 in red, and HS4 in green) were observed. The two doublets (HS1 and HS2) has Mössbauer parameters of $\delta = 0.97$ and $\Delta E_Q = 2.70\ mms^{-1}$ and $\delta = 0.93$ and $\Delta E_Q = 2.75\ mms^{-1}$, respectively, which correspond to HS Fe^{II} ions in the $[Fe_3(\mu_3\text{-}O)]$ core. The Mössbauer parameters of HS3 ($\delta = 1.13$ and $\Delta E_Q = 1.32\ mms^{-1}$) indicates that two apical Fe^{II} ions are in the HS state. The HS4 ($\delta = 0.36$ and $\Delta E_Q = 1.17\ mms^{-1}$) was assigned to HS Fe^{III} in the $[Fe_2OCl_6]^{2-}$ anion.[15b]

In summary, by introducing different counterions to the pentanuclear $\{Fe_5\}$ cluster compounds, the spin states of two apical iron(II) ions in the cationic pentanuclear $\{Fe_5\}$ clusters can be tuned in a HS state by an $[Fe_2OCl_6]^{2-}$ anion and in a LS state by a $SCN^-/ClO_4^-/I^-$ anion. Our studies provide an excellent example for the spin-transition cluster systems that exhibit a mixed-spin structures and synergy between spin transitions and magnetic interaction.

Experimental Section

Synthesis of 1: A solution of $FeCl_2{\cdot}4H_2O$ (0.039 g, 0.2 mmol), abpt (0.071 g, 0.3 mmol) and KNCS (0.039 g, 0.4 mmol) in distilled water (10 mL) was sealed in a 15 mL Teflon-lined reactor and heated at 160 °C for 3 days and then cooled to room temperature at 5 °C h^{-1}. Subsequently, red crystals were obtained in 33% yield based on Fe. IR (KBr): $\tilde{\nu} = 3411$ (s, br), 2911 (w), 2055 (m; NCS^-), 1604 (s), 1494 (w), 1463 (w), 1410 (m), 1384 (vs), 1155 (w), 1094 (w), 1039 (w), 1018 (w), 800 (w), 751 (w), 724 (m), 641 (w), 607 cm^{-1} (w); MS (ESI^+; CH_3OH): $m/z = 814.73$ [$\{Fe^{II}(\mu\text{-bpt})_3\}_2Fe^{II}_3(\mu_3\text{-}O)]^{2+}$; elemental analysis calcd (%) for **1**: C 46.17, H 3.56, N 23.29; found: C 44.42, H 4.08, N 22.42.

Synthesis of 2: A solution of $Fe(ClO_4)_2 \cdot 6H_2O$ (0.036 g, 0.1 mmol), abpt (0.029 g, 0.12 mmol), 1,2-di(4-pyridly)ethylene (0.036 g, 0.2 mmol), $NaNO_3 \cdot 3H_2O$ (0.027 g, 0.2 mmol) and triethylamine (0.012 g, 0.12 mmol) in methanol (10 mL) was sealed in a 15 mL Teflon-lined reactor and heated at 160 °C for 3 days before being cooled to room temperature at 5 °C h^{-1}. The precipitate was filtered off and the resulting red solution was allowed to stand for several days at room temperature and red crystals of **2** were isolated in about 7% yield based on Fe. IR (KBr): $\tilde{\nu}$ = 3406 (m), 3082 (w), 1606 (s), 1564 (w), 1492 (s), 1463 (m), 1409 (s), 1344 (w), 1274 (w), 1187 (w), 1092 (s), 1014 (w), 799 (m), 751 (m), 720 (m), 621 cm^{-1} (m); elemental analysis calcd (%) for **2**: C 45.96, H 2.89, N 22.33; found: C 46.67, H 3.16, N 22.20.

Synthesis of 3: A solution of $FeSO_4 \cdot 7H_2O$ (0.028 g, 0.1 mmol), abpt (0.029 g, 0.12 mmol), KI (0.033 g, 0.2 mmol) and triethylamine (0.012 g, 0.12 mmol) in acetonitrile (10 mL) was sealed in a 15 mL Teflon-lined reactor and heated at 160 °C for 3 days and was then cooled to room temperature at 5 °C h^{-1}. The precipitate was filtered off and the resulting red solution was allowed to stand several days at room temperature and red crystals of **3** were isolated in about 5% yield based on Fe. IR (KBr): $\tilde{\nu}$ = 3418 (m), 3066 (w), 1606 (s), 1565 (w), 1491 (m), 1461 (w), 1409 (s), 1276 (w), 1186 (w), 1150 (w), 1094 (w), 1043 (w), 1014 (w), 799 (m), 751 (m), 722 (s), 619 cm^{-1} (w).

Synthesis of 4: A solution of $FeCl_2 \cdot 4H_2O$ (0.020 g, 0.1 mmol), abpt (0.029 g, 0.12 mmol) and triethylamine (0.030 g, 0.3 mmol) in acetonitrile (10 mL) was sealed in a 15 mL Teflon-lined reactor and heated at 160 °C for 3 days and then cooled to room temperature at 5 °C h^{-1}. Subsequently, red crystals were obtained in 61% yield based on Fe. IR (KBr): 3408 (m), 3082 (w), 1605 (s), 1567 (w), 1496 (m), 1464 (m), 1411 (s), 1384 (m), 1340 (w), 1281 (w), 1187 (w), 1152 (w), 1092 (w), 1039 (m), 1016 (w), 872 (w), 780 (m), 745 (m), 725 (s), 704 (w), 643 cm^{-1} (w); MS (ESI$^+$; CH_3OH): m/z = 814.3 $[\{Fe^{II}(\mu\text{-bpt})_3\}_2Fe^{II}_3(\mu_3\text{-O})]^{2+}$; elemental analysis calcd (%) for **4**: C 43.72, H 2.50, N 21.24; found: C 43.73, H 2.829, N 21.54.

Crystal data of 1: At 100(2) K: $C_{74}H_{68}Fe_5N_{32}O_{11}S_2$; M_r = 1924.97 g mol^{-1}; tetragonal; space group $\bar{I}4$; a = 16.760(3), c = 29.442(7) Å; V = 8270(3) Å^3; Z = 4; ρ = 1.546 g cm^{-3}; θ_{max} = 27.36°; total data 35193; unique data 9291; μ = 0.986 mm^{-1}; 581 parameters; R_1 = 0.0749 for $[I \geq 2\sigma(I)]$ and wR_2 = 0.1996 for all data. At 293(2) K: a = 17.0404(8), c = 30.098(3) Å; V = 8739.6(10) Å^3; Z = 4; ρ = 1.463 g cm^{-3}; θ_{max} = 27.49°; total data 15954; unique data 8238; μ = 0.933 mm^{-1}; 555 parameters; R_1 = 0.0693 for $[I \geq 2\sigma(I)]$ and wR_2 = 0.2068 for all data.

Crystal data of 2: At 150(2) K: $C_{72}H_{54}Fe_5N_{30}O_{12}Cl_2$, M_r = 1881.60 g mol^{-1}; monoclinic; space group $P2_1/n$; a = 12.4271(7), b = 12.8685(6), c = 48.514(2) Å; β = 94.231(2)°; V = 7737.1(7) Å^3; Z = 4; ρ = 1.615 g cm^{-3}; θ_{max} = 27.00°; total data 38089; unique data 16197; μ = 1.067 mm^{-1}; 1103 parameters; R_1 = 0.1012 for $[I \geq 2\sigma(I)]$ and wR_2 = 0.3574 for all data. At 308(2) K: $C_{72}H_{48}Fe_5N_{30}O_9Cl_2$; a = 12.4294(6), b = 12.8798(6), c = 48.175(2) Å; β = 94.003(1)°; V = 7693.4(6) Å^3; Z = 4, ρ = 1.578 g cm^{-3}; θ_{max} = 27.00°; total data 44188; unique data 16160 μ = 1.068 mm^{-1}; 1053 parameters; R_1 = 0.0943 for $[I \geq 2\sigma(I)]$ and wR_2 = 0.3289 for all data.

Crystal data of 3: At 150(2) K: $C_{80}H_{60}Fe_5N_{34}OI_2$; M_r = 2046.67 g mol^{-1}; monoclinic; space group $C2/c$; a = 20.6573(8), b = 14.4428(8), c = 27.1360(10) Å; β = 90.341(2)°; V = 8095.9(6) Å^3; Z = 4; ρ = 1.679 g cm^{-3}; θ_{max} = 26.50°; total data 21724; unique data 7997; μ = 1.708 mm^{-1}; 542 parameters; R_1 = 0.0684 for $[I \geq 2\sigma(I)]$ and wR_2 = 0.1513 for all data. At 293(2) K: a = 19.154(6), b = 15.960(5), c = 25,802(8) Å; β = 96.076(5)°; V = 7789(4) Å^3; Z = 4, ρ = 1.745 g cm^{-3}; θ_{max} = 26.00°; total data 13639; unique data 7160; μ = 1.775 mm^{-1}; 498 parameters R_1 = 0.0969 (squeeze) for $[I \geq 2\sigma(I)]$ and wR_2 = 0.2817 (squeeze) for all data.

Crystal data of 4: At 100(2) K: $C_{72}H_{49}Cl_6Fe_7N_{30}O_{2.5}$; M_r = 1978.06 g mol^{-1}; monoclinic; space group $P2_1/c$; a = 20.8143(6), b = 17.5001(6), c = 22.2571(7) Å; β = 99.318(1)°; V = 8000.2(4) Å^3; Z = 4; ρ = 1.642 g cm^{-3}; θ_{max} = 27.44°; total data 75768; unique data 18124; μ = 1.501 mm^{-1}; 1063 parameters; R_1 = 0.0612 for $[I \geq 2\sigma(I)]$ and wR_2 = 0.1639 for all data. At 290(2) K: a = 20.8973(7), b = 17.5798(6), c = 22.6267(9) Å; β = 99.170(1)°; V = 8206.1(5) Å^3; Z = 4; ρ = 1.594 g cm^{-3}; θ_{max} = 27.00°; total data 45208; unique data 17232; μ = 1.463 mm^{-1}; 1055 parameters; R_1 = 0.0649 for $[I \geq 2\sigma(I)]$ and wR_2 = 0.2119 for all data.

The intensity data were recorded on a Bruker SMART Apex CCD system with $Mo_{K\alpha}$ radiation (λ = 0.71073 Å). The structure was solved by direct methods and refined on F^2 by using SHELXTL. CCDC-764245 (**1**) 764246 (**2**) 764247 (**3**) 764248 (**4**) contain the supplementary crystallographic data for this paper. These data can be obtained free of charge from The Cambridge Crystallographic Data Centre via www.ccdc.cam.ac.uk/data_request/cif.

Magnetic susceptibility measurements of **1** and **4** were performed on a Quantum Design MPMS-XL7 SQUID. The diamagnetic correction for each sample was determined from Pascal's constants.

Mössbauer experiments were carried out by using a ^{57}Co/Rh source in a constant-acceleration transmission spectrometer. The spectra were recorded at 20 K in both cooling and heating modes. The spectrometer was calibrated by using a standard α-Fe foil.

Acknowledgements

This work was supported by the NSFC (Grant no. 20525102, 20821001, 90922009, J0730420 and 50872157) and the "973 Project" (2007CB815305).

Keywords: cluster compounds · iron · magnetic properties · spin transitions · triazoles

[1] a) O. Kahn, C. J. Martinez, *Science* **1998**, *279*, 44–48; b) P. Gütlich, A. Hauser, H. Spiering, *Angew. Chem.* **1994**, *106*, 2109–2141; *Angew. Chem. Int. Ed. Engl.* **1994**, *33*, 2024–2054; c) J. A. Real, A. B. Gaspar, V. Niel, M. C. Muñoz, *Coord. Chem. Rev.* **2003**, *236*, 121–141; d) J. F. Létard, P. Guionneau, L. Goux-Capes, *Topics in Current Chemistry, Vol. 235*, Springer, Heidelberg, **2004**, pp. 221–249; e) A. Galet, A. B. Gaspar, M. C. Muñz, G. V. Bukin, G. Levchenko, J. A. Real, *Adv. Mater.* **2005**, *17*, 2949–2953; f) M. Cavallini, I. Bergenti, S. Milita, G. Ruani, I. Salitros, Z.-R. Qu, R. Chandrasekar, M. Ruben, *Angew. Chem.* **2008**, *120*, 8724–8728; *Angew. Chem. Int. Ed.* **2008**, *47*, 8596–8600; g) P. Gamez, J. S. Costa, M. Quesada, G. Aromí, *Dalton Trans.* **2009**, 7845–7853.

[2] a) A. Bousseksou, G. Molnár, G. Matouzenko, *Eur. J. Inorg. Chem.* **2004**, 4353–4369; b) J. A. Real, A. B. Gaspar, M. C. Muñoz, *Dalton Trans.* **2005**, 2062–2079; c) J. A. Kitchen, S. Brooker, *Coord. Chem. Rev.* **2008**, *252*, 2072–2092.

[3] a) M. Seredyuk, A. B. Gaspar, V. Ksenofontov, M. Verdaguer, F. Villain, P. Gütlich, *Inorg. Chem.* **2009**, *48*, 6130–6141; b) M. Bartel, A. Absmeier, G. N. L. Jameson, F. Werner, K. Kato, M. Takata, R. Boca, M. Hasegawa, K. Mereiter, A. Caneschi, W. Linert, *Inorg. Chem.* **2007**, *46*, 4220–4229; c) M. Nihei, L. Han, H. Oshio, *J. Am. Chem. Soc.* **2007**, *129*, 5312–5313; d) A. Galet, M. C. Muñoz, J. A. Real, *Chem. Commun.* **2006**, 4321–4323; e) V. Niel, A. L. Thompson, M. C. Muñoz, A. Galet, A. E. Goeta, J. A. Real, *Angew. Chem.* **2003**, *115*, 3890–3893; *Angew. Chem. Int. Ed.* **2003**, *42*, 3760–3763; f) S. M. Neville, G. J. Halder, K. W. Chapman, M. B. Duriska, P. D. Southon, J. D. Cashion, J.-F. Létard, B. Moubaraki, K. S. Murray, C. J. Kepert, *J. Am. Chem. Soc.* **2008**, *130*, 2869–2876; g) G. J. Halder, K. W. Chapman, S. M. Neville, B. Moubaraki, K. S. Murray, J.-F. Létard, C. J. Kepert, *J. Am. Chem. Soc.* **2008**, *130*, 17552–17562.

[4] a) G. S. Matouzenko, A. Bousseksou, S, Lecocq, P. J. van Koningsbruggen, M. Perrin, O. Kahn, A. Collet, *Inorg. Chem.* **1997**, *36*, 5869–5879; b) S. M. Neville, B. A. Leita, D. A. Offermann, M. B. Duriska, B. Moubaraki, K. W. Chapman, G. J. Halder, K. S. Murray, *Eur. J. Inorg. Chem.* **2007**, 1073–1085; c) D. L. Reger, J. R. Gardinier, M. D. Smith, A. M. Shahin, G. J. Long, L. Rebbouh, F. Grandjean, *Inorg. Chem.* **2005**, *44*, 1852–1866; d) A. L. Thompson, A. E. Goeta, J. A. Real, A. Galet, M. C. Muñoz, *Chem. Commun.* **2004**, 1390–1391.

[5] a) M. Yamada, M. Ooidemizu, Y. Ikuta, S. Osa, N. Matsumoto, S. Iijima, M. Kojima, F. Dahan, J.-P. Tuchagues, *Inorg. Chem.* **2003**, *42*, 8406–8416; b) M. Seredyuk, A. B. Gaspar, M. C. Muñoz, M. Verdaguer, F. Villain, P. Gütlich, *Eur. J. Inorg. Chem.* **2007**, 4481–4491; c) D. Chernyshov, M. Hostettler, K. W. Törnroos, H.-B. Bürgi, *Angew. Chem.* **2003**, *115*, 3955–3960; *Angew. Chem. Int. Ed.* **2003**, *42*, 3825–3830; d) B. Weber, E. Kaps, J. Weigand, C. Carbonera, J.-F. Létard, K. Achterhold, F. G. Parak, *Inorg. Chem.* **2008**, *47*, 487–496; e) J. A. Kitchen, N. G. White, M. Boyd, B. Moubaraki, K. S. Murray, P. D. W. Boyd, S. Brooker, *Inorg. Chem.* **2009**, *48*, 6670–6679; f) C. Rajadurai, Z, Qu, O. Fuhr, B. Gopalan, R. Kruk, M. Ghafari, M. Ruben, *Dalton Trans.* **2007**, 3531–3537; g) M. Yamada, H. Hagiwara, H. Torigoe, N. Matsumoto, M. Kojima, F. Dahan, J.-P. Tuchagues, N. Re, S. Iijima, *Chem. Eur. J.* **2006**, *12*, 4536–4549.

[6] a) P. Gütlich, Y. Garcia, H. A. Goodwin, *Chem. Soc. Rev.* **2000**, *29*, 419–427; b) O. Sato, J. Tao, Y.-Z. Zhang, *Angew. Chem.* **2007**, *119*, 2200–2236; *Angew. Chem. Int. Ed.* **2007**, *46*, 2152–2187; c) K. S. Murray, *Eur. J. Inorg. Chem.* **2008**, 3101–3121; d) B. Weber, *Coord. Chem. Rev.* **2009**, *253*, 2432–2449; e) J. A. Real, A. B. Gaspar, V. Niel, M. C. Muñoz, *Coord. Chem. Rev.* **2003**, *236*, 121–141.

[7] a) J. F. Létard, J. A. Real, N. Moliner, A. B. Gasper, L. Capes, O. Cador, O. Kahn, *J. Am. Chem. Soc.* **1999**, *121*, 10630–10631; b) G. Chastanet, A. B. Gaspar, J. A. Real, J. F. Létard, *Chem. Commun.* **2001**, 819–820; c) G. Chastanet, C. Carbonera, C. Mingotaud, J. F. Létard, *J. Mater. Chem.* **2004**, *14*, 3516–3523; d) S. Hayami, G. Juhász, Y. Maeda, T. Yokoyama, O. Sato, *Inorg. Chem.* **2005**, *44*, 7289–7291; e) S. Brooker, P. G. Plieger, B. Moubaraki, K. S. Murray, *Angew. Chem.* **1999**, *111*, 424–426; *Angew. Chem. Int. Ed.* **1999**, *38*, 408–410; f) M. Arai, W. Kosaka, T. Matsuda, S.-i. Ohkoshi, *Angew. Chem.* **2008**, *120*, 6991–6993; *Angew. Chem. Int. Ed.* **2008**, *47*, 6885–6887.

[8] a) M.-X. Peng, C.-G. Hong, C.-K. Tan, J.-C. Chen, M.-L. Tong, *J. Chem. Crystallogr.* **2006**, *36*, 703–707; b) J.-C. Chen, S. Hu, A.-J. Zhou, M.-L. Tong, Y.-X. Tong, *Z. Anorg. Allg. Chem.* **2006**, *632*, 475–481; c) M.-L. Tong, C.-G. Hong, L.-L. Zheng, M.-X. Peng, A. Gaita-Ariño, J. M. Clemente Juan, *Eur. J. Inorg. Chem.* **2007**, 3710–3717; d) Z.-S. Meng, L. Yun, W.-X. Zhang, C.-G. Hong, R. Herchel, Y.-C. Ou, J.-D. Leng, M.-X. Peng, Z. Lin, M.-L. Tong, *Dalton Trans.* **2009**, 10284–10295; e) K. Yoneda, K. Adachi, K. Nishio, M. Yamasaki, A. Fuyuhiro, M. Katada, S. Kaizaki, S. Kawata, *Angew. Chem.* **2006**, *118*, 5585–5587; *Angew. Chem. Int. Ed.* **2006**, *45*, 5459–5461.

[9] G. Agustí, S. Cobo, A. B. Gaspar, G. Molnár, N. O. Moussa, P. Á. Szilágyi, V. Pálfi, C. Vieu, M. C. Muñoz, J. A. Real, A. Bousseksou, *Chem. Mater.* **2008**, *20*, 6721–6732.

[10] M. Clemente-León, E. Coronado, M. C. Giménez-López, F. M. Romero, *Inorg. Chem.* **2007**, *46*, 11266–11276.

[11] P. Guionneau, M. Marchivie, G. Bravic, J.-F. Létard, D. Chasseau, *J. Mater. Chem.* **2002**, *12*, 2546–2551.

[12] a) J.-F. Létard, P. Guionneau, L. Rabardel, J. A. K. Howard, A. E. Goeta, D. Chasseau, O. Kahn, *Inorg. Chem.* **1998**, *37*, 4432–4441; b) S. Bonnet, G. Molnár, J. S. Costa, M. A. Siegler, A. L. Spek, A. Bousseksou, W.-T. Fu, P. Gamez, J. Reedijk, *Chem. Mater.* **2009**, *21*, 1123–1136; c) J. S. Costa, K. Lappalainen, G. de Ruiter, M. Quesada, J. Tang, I. Mutikainen, U. Turpeinen, C. M. Grunert, P. Gü1tlich, H. Z. Lazar, J.-F. Létard, P. Gamez, J. Reedijk, *Inorg. Chem.* **2007**, *46*, 4079–4089.

[13] O. Kahn, *Molecular Magnetism*, Wiley-VCH, New York, **1993**.

[14] a) M. Viciano-Chumillas, S. Tanase, I. Mutikainen, U. Turpeinen, L. J. de Jongh, J. Reedijk, *Inorg. Chem.* **2008**, *47*, 5919–5929; b) J. Tao, Y. Z. Zhang, Y. L. Bai, O. Sato, *Inorg. Chem.* **2006**, *45*, 4877–4879; c) Y. L. Bai, J. Tao, W. Wernsdorfer, O. Sato, R. B. Huang, L. S. Zheng, *J. Am. Chem. Soc.* **2006**, *128*, 16428–16429; d) H. B. Xu, B. W. Wang, F. Pan, Z. M. Wang, S. Gao, *Angew. Chem.* **2007**, *119*, 7532–7536; *Angew. Chem. Int. Ed.* **2007**, *46*, 7388–7393; e) C. M. Liu, D. Q. Zhang, D. B. Zhu, *Chem. Commun.* **2008**, 368–370.

[15] a) G. Haselhorst, K. Wieghardt, S. Keller, B. Schrade, *Inorg. Chem.* **1993**, *32*, 520–525; b) Y. Lan, D. K. Kennepohl, B. Moubaraki, K. S. Murray, J. D. Cashion, G. B. Jameson, S. Brooker, *Chem. Eur. J.* **2003**, *9*, 3772–3784.

[16] a) F. Pointillart, K. Bernot, R. Sessoli, D. Gatteschi, *Chem. Eur. J.* **2007**, *13*, 1602–1609; b) W. Shi, X.-Y. Chen, B. Zhao, A. Yu, H.-B. Song, P. Cheng, H.-G. Wang, D.-Z. Liao, S.-P. Yan, *Inorg. Chem.* **2006**, *45*, 3949–3957; c) M. L. Kahn, C. Mathonière, O. Kahn, *Inorg. Chem.* **1999**, *38*, 3692–3697; d) M. L. Kahn, P. Lecante, M. Verelst, C. Mathonière, O. Kahn, *Chem. Mater.* **2000**, *12*, 3073–3079.

[17] a) J. Elhaïk, D. J. Evans, C. A. Kilner, M. A. Halcrow, *Dalton Trans.* **2005**, 1693–1700; b) R. Boča, *Coord. Chem. Rev.* **2004**, *248*, 757–815.

Received: March 1, 2010
Published online: April 21, 2010

